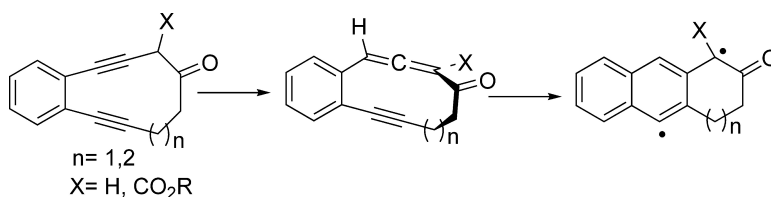


Enhancement of the Reactivity of Photochemically Generated Eneidyne via Keto#Enol Tautomerization

Grigori Karpov, Alexander Kuzmin, and Vladimir V. Popik

J. Am. Chem. Soc., **2008**, 130 (35), 11771-11777 • DOI: 10.1021/ja802688c • Publication Date (Web): 09 August 2008

Downloaded from <http://pubs.acs.org> on February 8, 2009



More About This Article

Additional resources and features associated with this article are available within the HTML version:

- Supporting Information
- Links to the 1 articles that cite this article, as of the time of this article download
- Access to high resolution figures
- Links to articles and content related to this article
- Copyright permission to reproduce figures and/or text from this article

[View the Full Text HTML](#)

Enhancement of the Reactivity of Photochemically Generated Eneidyne via Keto–Enol Tautomerization

Grigori Karpov, Alexander Kuzmin, and Vladimir V. Popik*

Department of Chemistry, University of Georgia, Athens, Georgia 30602

Received April 16, 2008; E-mail: vpopik@uga.edu

Abstract: Ten- and eleven-membered-ring cyclic eneidyne that possess a carbonyl group in a β position with respect to the one of acetylenic termini undergo very facile cycloaromatization at ambient temperatures. Kinetic data and deuterium-labeling experiments indicate that this reaction proceeds via rate-determining tautomerization to the allene–ene-yne form followed by very rapid Myers–Saito cyclization.

Introduction

The extreme antineoplastic activity of natural eneidyne antibiotics¹ is attributed to the ability of the (Z)-3-hexene-1,5-diyne² and (Z)-1,2,4-heptatrien-6-yne³ fragments to undergo cycloaromatization and produce dDNA-damaging aromatic diradicals.^{1,4} Lack of antitumor selectivity, which results in a very high general toxicity, hampers clinical applications of natural eneidyne antibiotics.⁵ Photochemical triggering of the cycloaromatization reaction might help to alleviate this problem by allowing for spatial and temporal control of eneidyne reactivity.⁶ The direct irradiation of acyclic⁷ and cyclic⁸ eneidyne and of the natural eneidyne antibiotic Dynemicin A⁹ demonstrated that the Bergman cyclization can be induced photochemically, albeit with low efficiency. The quantum yield of the photochemical Bergman cyclization can be substantially

improved by adjusting the electronic properties of substituents¹⁰ and/or using different modes of excitation energy transfer, such as metal-to-ligand charge transfer.¹¹ In addition, several caged eneidyne that undergo conventional chemical activation after the photochemical uncaging step have been prepared.¹²

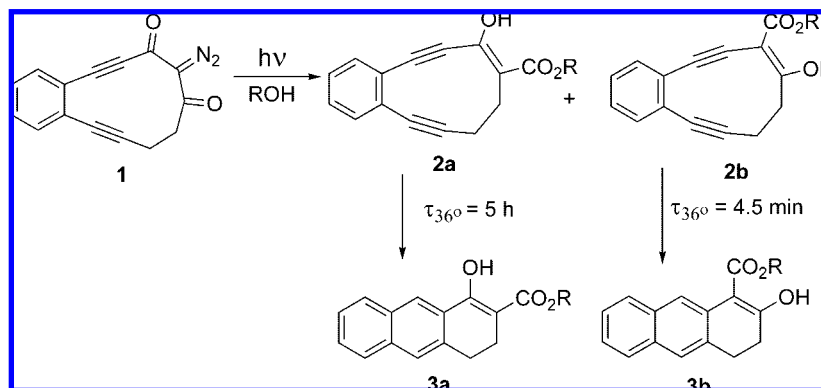
Our group has explored an alternative strategy for the phototriggering of the cycloaromatization reaction: in situ generation of an activated eneidyne system.¹³ We have designed eneidyne precursors that are stable in the dark but efficiently converted into reactive form upon irradiation with UV–vis¹⁴ or near-infrared (NIR)¹⁵ light. To exploit the benefits of this strategy, photogenerated eneidyne should undergo very rapid cyclization at ambient temperature. In our preliminary communication,^{14a} we reported the photochemical generation of reactive isomeric 10-membered-ring eneidyne **2a** and **2b** from thermally stable (below 80 °C) diazodiketone precursor **1** (Scheme 1).

While facile cycloaromatization of these 3,4-benzocyclodeca-1,5-diyne derivatives under ambient conditions is remarkable,¹⁶ the almost 70-fold difference in the rates of cycloaromatization of the two regioisomeric eneidyne **2a** and **2b** is even more

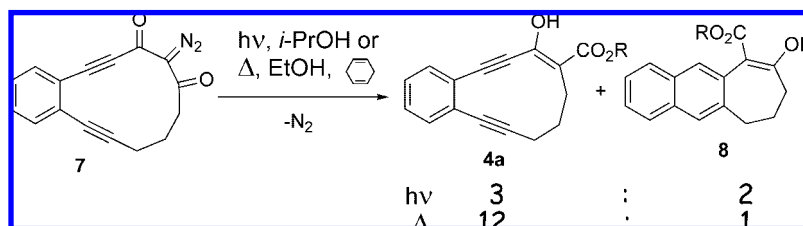
- (1) *Eneidyne Antibiotics as Antitumor Agents*; Borders, D. B., Doyle, T. W., Eds.; Marcel Dekker: New York, 1995.
- (2) Bergman, R. G. *Acc. Chem. Res.* **1973**, *6*, 25.
- (3) (a) Myers, A. G.; Kuo, E. Y.; Finnney, N. S. *J. Am. Chem. Soc.* **1989**, *111*, 8057. (b) Nagata, R.; Yamanaka, H.; Okazaki, E.; Saito, I. *Tetrahedron Lett.* **1989**, *30*, 4995. (c) Myers, A. G.; Dragovich, P. S.; Kuo, E. Y. *J. Am. Chem. Soc.* **1992**, *114*, 9369.
- (4) (a) For recent reviews, see: Danishefsky, S. J.; Shair, M. D. *J. Org. Chem.*, **1996**, *61*, 16. (b) Nicolaou, K. C.; Dai, W.-M. *Angew. Chem., Int. Ed. Engl.* **1991**, *30*, 1387. (c) Thorson, J. S.; Ahlert, J.; Shepard, E.; Whitwam, R. E.; Onwueme, K. C.; Sievers, E. L.; Ruppen, M. *Curr. Pharm. Des.* **2000**, *6*, 1841.
- (5) (a) Galm, U.; Hager, M. H.; Lanen, S. G. V.; Ju, J.; Thorson, J. S.; Shen, B. *Chem. Rev.* **2005**, *105*, 739. (b) Gredicak, M.; Jeric, I. *Acta Pharm.* **2007**, *57*, 133. (c) Shen, B.; Nonaka, K. *Curr. Med. Chem.* **2003**, *10*, 2317.
- (6) (a) Kar, M.; Basak, A. *Chem. Rev.* **2007**, *107*, 2861. (b) Jones, G. B.; Fouad, F. S. *Curr. Pharm. Des.* **2002**, *8*, 2415.
- (7) (a) Kagan, J.; Wang, X.; Chen, X.; Lau, K. Y.; Batac, I. V.; Tuveson, R. W.; Hudson, J. B. *J. Photochem. Photobiol., B* **1993**, *21*, 135. (b) Turro, N. J.; Evenzahav, A.; Nicolaou, K. C. *Tetrahedron Lett.* **1994**, *35*, 8089. (c) Kaneko, T.; Takahashi, M.; Hiram, M. *Angew. Chem., Int. Ed.* **1999**, *38*, 1267. (d) Plourde, G.; El-Shafey, A.; Fouad, F.; Purohit, A.; Jones, G. *Bioorg. Med. Chem. Lett.* **2002**, *12*, 2985. (e) Falcone, D.; Li, J.; Kale, A.; Jones, G. B. *Bioorg. Med. Chem. Lett.* **2008**, *18*, 934. (f) Spence, J. D.; Hargrove, A. E.; Crampton, H. L.; Thomas, D. W. *Tetrahedron Lett.* **2007**, *48*, 725. (g) Sud, D.; Wigglesworth, T. J.; Branda, N. R. *Angew. Chem., Int. Ed.* **2007**, *46*, 8071.
- (8) (a) Choy, N.; Blanco, B.; Wen, J.; Krishan, A.; Russell, K. C. *Org. Lett.* **2000**, *2*, 3761. (b) Funk, R. L.; Young, E. R. R.; Williams, R. M.; Flanagan, M. F.; Cecil, T. L. *J. Am. Chem. Soc.* **1996**, *118*, 3291.
- (9) Shiraki, T.; Sugiura, Y. *Biochemistry* **1990**, *29*, 9795.

- (10) (a) Alabugin, I. V.; Manoharan, M. *J. Phys. Chem. A* **2003**, *107*, 3363. (b) Alabugin, I. V.; Manoharan, M.; Kovalenko, S. V. *Org. Lett.* **2002**, *4*, 1119. (c) Clark, A. E.; Davidson, E. R.; Zaleski, J. M. *J. Am. Chem. Soc.* **2001**, *123*, 2650.
- (11) (a) Benites, P. J.; Holmberg, R. C.; Rawat, D. S.; Kraft, B. J.; Klein, L. J.; Peters, D. G.; Thorp, H. H.; Zaleski, J. M. *J. Am. Chem. Soc.* **2003**, *125*, 6434. (b) Kraft, B. J.; Coalter, N. L.; Nath, M.; Clark, A. E.; Siedle, A. R.; Huffman, J. C.; Zaleski, J. M. *Inorg. Chem.* **2003**, *42*, 1663. (c) Bhattacharyya, S.; Pink, M.; Baik, M. H.; Zaleski, J. M. *Angew. Chem., Int. Ed.* **2005**, *44*, 592.
- (12) (a) Nicolaou, K. C.; Dai, W.-M.; Wendeborn, S. V.; Smith, A. L.; Torisawa, Y.; Malignes, P.; Hwang, C.-K. *Angew. Chem., Int. Ed. Engl.* **1991**, *30*, 1032. (b) Nicolaou, K. C.; Dai, W.-M. *J. Am. Chem. Soc.* **1992**, *114*, 8908. (c) Wender, P. A.; Zercher, C. K.; Beckham, S.; Haubold, E.-M. *J. Org. Chem.* **1993**, *58*, 5867. (d) Wender, P. A.; Beckham, S.; O'Leary, J. G. *Synthesis* **1994**, 1278. (e) Basak, A.; Bdoor, H. M.; Shain, J. C.; Mandal, S.; Rudra, K. R.; Nag, S. *Bioorg. Med. Chem. Lett.* **2000**, *10*, 1321.
- (13) Poloukhine, A.; Karpov, G.; Popik, V. V. *Curr. Trends Med. Chem.* **2008**, *8*, 460.
- (14) (a) Karpov, G.; Popik, V. V. *J. Am. Chem. Soc.* **2007**, *129*, 3792. (b) Poloukhine, A.; Popik, V. V. *J. Org. Chem.* **2005**, *70*, 1297. (c) Poloukhine, A.; Popik, V. V. *Chem. Commun.* **2005**, 617.
- (15) Poloukhine, A.; Popik, V. V. *J. Org. Chem.* **2006**, *71*, 7417.
- (16) The parent 3,4-benzocyclodeca-1,5-diyne and other known derivatives are stable under ambient conditions; see: Semmelhack, M. F.; Neu, T.; Foubelo, F. *J. Org. Chem.* **1994**, *59*, 5038.

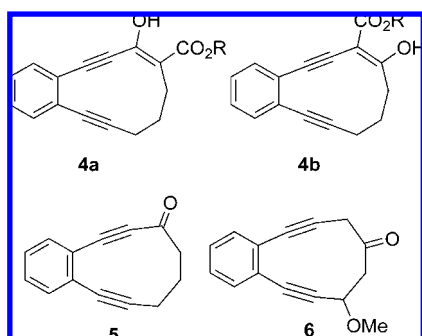
Scheme 1



Scheme 2



intriguing. To gain an understanding of the origin of this difference, we undertook a detailed study of the mechanisms of cyclization of ketoesters **2a** and **2b**, their 11-membered-ring analogues **4a** and **4b**, and the model 10-membered-ring enediyne **5** and **6**.



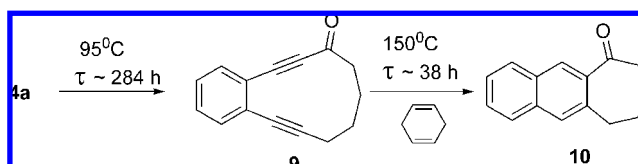
Results and Discussion

Generation and Reactivity of Eleven-Membered-Ring Enediyne Ketoesters **4a and **4b**.** The twelve-membered-ring 2-diazo-1,3-diketone **7** was prepared using synthetic procedures similar to those for the preparation of **1**.^{14a,17} Irradiation of **7** in alcohols was expected to produce the target 11-membered-ring enediyne ketoesters **4a** and **4b** via the photo-Wolff reaction. Since the parent 3,4-benzocycloundeca-1,5-diyne and cycloundeca-3-ene-1,5-diyne show no signs of decomposition up to 84 °C,¹⁸ we expected **4a** and **4b** to be stable under ambient conditions. Photolysis of diazodiketone **7** in 2-propanol at 25 °C with 350 nm light resulted in efficient consumption of the starting material ($\Phi_{350\text{nm}} = 0.22 \pm 0.02$) and the formation of two major products.

Separation of the reaction mixture produced only one of the expected enediyne ketoesters, **4a** (R = *i*-Pr), along with isopropyl 7,8-dihydro-10-hydroxy-6*H*-cyclohepta[*b*]naphthalene-7-carboxylate (**8**, R = *i*-Pr) in a 3:2 ratio (Scheme 2). The latter compound is an apparent product of the Bergman cyclization of the regioisomeric enediyne **4b**. Similar products were obtained upon heating of **7** in an ethanol/cyclohexadiene mixture at 92 °C for 3 h. The product ratio of the thermolysis was shifted even further in favor of **4a** (R = Et) (Scheme 2).

Both of the β -ketoesters (**4a** and **8**) were fully enolized according to NMR data.¹⁷ As we anticipated, 11-membered-ring enediyne **4a** is perfectly stable below 80 °C and undergoes slow decomposition only at elevated temperatures. In fact, heating of **4a** in neat, argon-purged cyclohexadiene did not result in the direct Bergman cyclization but rather in decarboxylation of the starting material to give 4,5-benzocycloundeca-2,6-diyne (**9**). The latter requires even higher temperatures to induce cycloaromatization, yielding naphthalene derivative **10** (Scheme 3).

Scheme 3



In sharp contrast with **4a**, regioisomeric 11-membered-ring enediyne **4b** is not stable enough even at 0 °C to survive separation procedures; β -ketoester **8** was always isolated instead. To measure the rate of cycloaromatization of **4b**, 2-diazo-1,3-diketone **7** was photolyzed in 2-propanol at 0 °C to $\sim 90\%$ conversion. Immediate HPLC analysis of the reaction mixture showed the presence of three major products (in addition to unreacted **7**): ketoesters **4a** and **8** as well as an unknown compound. When the mixture was left to stand in the dark at room temperature, the integral intensity of the peak corresponding to the unknown

(17) See the Supporting Information for details.

(18) Semmelhack, M. F.; Neu, T.; Foubelo, F. *Tetrahedron Lett.* **1992**, 33, 3277.

compound decreased while the concentration of **8** rose at the same rate. This observation allowed us to conclude that the unknown compound was the unstable enediyne **4b**. The accurate rate measurements of **4b** cyclization were conducted using UV spectroscopy, following the growth of the characteristic 322 nm band of **8** in the photolysate at 36 ± 0.1 °C (Figure 1). The reaction followed first-order kinetics well, as shown in the inset of Figure 1. The lifetime of enediyne **4b** was only 40 min at 36 °C. To the best of our knowledge, this is the first reported example of eleven-membered-ring enediyne that undergoes spontaneous Bergman cyclization under ambient conditions.

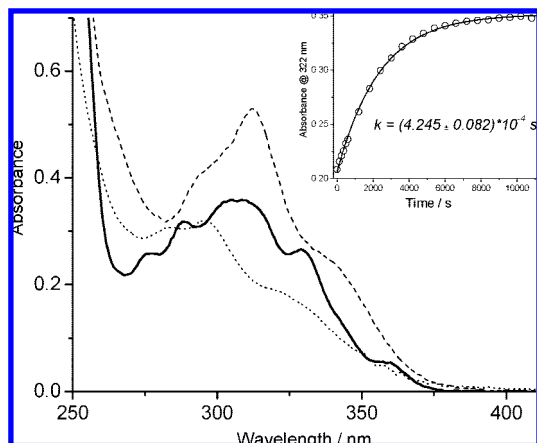


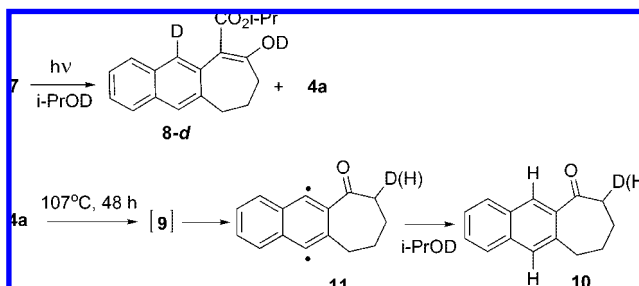
Figure 1. UV spectra of an $\sim 3 \times 10^{-5}$ M 2-propanol solution of **7** (dashed line) before and (dotted line) after 350 nm irradiation. The solid line represents the spectrum of an $\sim 3 \times 10^{-5}$ M solution of **8** in 2-propanol. The inset shows the growth in absorbance at 322 nm after irradiation of **7**. The line shown in the inset was drawn using parameters obtained by least-squares fitting of a single-exponential equation.

The difference in the reactivities of **4a** and **4b** resembles the difference observed for **2a** and **2b**, but it is much more pronounced.^{14a} We hypothesized that this dramatic difference in the rates of cycloaromatization stems from the different cyclization mechanisms of regioisomeric enediynes **4a** and **4b** as well as of **2a** and **2b**. Deuterium-incorporation experiments provided initial support for this suggestion. While heating of **4a** in 2-propanol-*d*₁ [(CH₃)₂CHOD] produced ketone **10** with no observable deuteration in the naphthalene ring, irradiation of diazo precursor **7** in 2-propanol-*d*₁ produced 7,8-dihydro-6*H*-cyclohepta[*b*]naphthalene derivative **8-d**, which is fully deuterated at the 11 position (Scheme 4). Incorporation of deuterium in this position apparently contradicts the Bergman mechanism, which should proceed via formation of the aromatic 6,11-diradical intermediate. A substituted *p*-benzyl diradical such as **11** (Scheme 4) is expected to preferentially abstract protium from the secondary carbon of (CH₃)₂CHOD, as observed for **4a** (see below), because this C–H bond is much weaker than the O–D bond.

The rate of formation of the product **8** and the rate of cyclization of **2b** are also strongly affected by the isotopic substitution in the solvent. Both reactions were substantially slower in 2-propanol-*d*₁, showing the normal primary kinetic isotope effect: $k_{\text{H}}/k_{\text{D}} = 3.20$ and 2.18 for **2b** and **4b**, respectively. These observations indicate that transfer of the hydroxylic proton (deuteron) is involved in the rate-limiting step of the reaction.

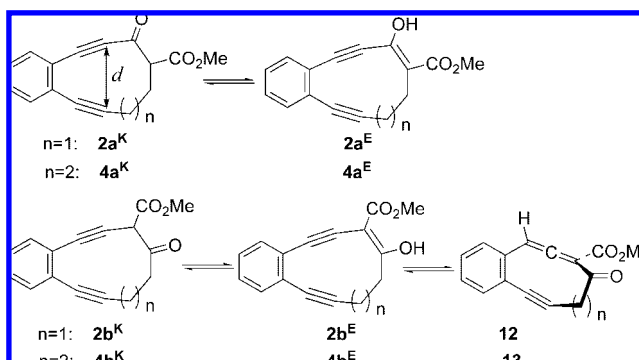
Theoretical Analysis. Theoretical analysis of the structural properties and tautomeric equilibria of β -ketoesters **2a** and **2b** (R = Me) and **4a** and **4b** (R = Me) (Scheme 5) was conducted at the B3LYP/6-311++G(d,p)//B3LYP/6-31++G(d,p) and FC-

Scheme 4



MP2/6-31++G(d,p)//B3LYP/6-31++G(d,p) levels of theory. The optimized geometries of structures **2a**, **2b**, **4a**, **4b**, **12**, and **13** as well as details concerning the theoretical procedures are provided in the Supporting Information. The relative electronic energies of tautomers of 10- and 11-membered-ring enediynes as well as ring-strain energies for 10-membered-ring isomers are shown in Table 1. This table also lists the transannular distance (i.e., the distance *d* between the acetylenic termini, as shown in Scheme 5) for each of the enediyne structures. While the barrier for the Bergman reaction of cyclic enediynes depends on many factors,^{10a,19} the release of ring strain in the transition state is one of the most important.²⁰ Values of *d* within groups of structurally similar enediynes correlate well with the latter and therefore can be predictive of reactivity.²¹

Scheme 5



NMR data for the more stable isomers (**2a** and **4a**) indicate that β -ketoester moieties of both enediynes exist predominantly in an enol form.^{14a,17} This observation agrees well with second-order Møller–Plesset perturbation theory (MP2) and especially density functional theory (DFT) results (Table 1). The relative energies of the enol tautomers become even lower for reactive regioisomers **2b** and **4b**, suggesting that these molecules also are fully enolized. It is interesting to note that the increase in

- (19) (a) Rawat, D. S.; Zaleski, J. M. *Synlett* **2004**, 393. (b) Jones, G. B.; Wright, J. M.; Hynd, G.; Wyatt, J.; Warner, P. M.; Huber, R. S.; Li, A.; Kilgore, M. W.; Sticca, R. P.; Pollenz, R. S. *J. Am. Chem. Soc.* **2001**, *123*, 2134. (c) Prall, M.; Wittkopp, A.; Fokin, A. A.; Schreiner, P. R. *J. Comput. Chem.* **2001**, *22*, 1605. (d) Schreiner, P. R. *J. Am. Chem. Soc.* **1998**, *120*, 4184. (e) Alabugin, I. V.; Manoharan, M. *J. Phys. Chem. A* **2003**, *107*, 3363.
- (20) (a) Snyder, J. P. *J. Am. Chem. Soc.* **1990**, *112*, 5367. (b) Magnus, P.; Fort, S.; Pitterna, T.; Snyder, J. P. *J. Am. Chem. Soc.* **1990**, *112*, 4986. (c) Brandstetter, T.; Maier, M. E. *Tetrahedron* **1994**, *50*, 1435.
- (21) (a) Jones, G. B.; Wright, J. M.; Hynd, G.; Wyatt, J.; Warner, P. M.; Huber, R. S.; Li, A.; Kilgore, M. W.; Sticca, R. P.; Pollenz, R. S. *J. Org. Chem.* **2002**, *67*, 5727. (b) Gaffney, S. M.; Capitani, J. F.; Castaldo, L.; Mitra, A. *Int. J. Quantum Chem.* **2003**, *95*, 706. (c) Chen, W.-C.; Zou, J.-W.; Yu, C.-H. *J. Org. Chem.* **2003**, *68*, 3663.

Table 1. Relative Electronic Energies (ΔE) and Transannular Distances (d) for Keto (K) and Enol (E) Forms of 10-Membered-Ring (**2a**, **2b**) and 11-Membered-Ring (**4a**, **4b**) Eneidyne- β -ketoesters and for the Corresponding Allene–Eneyne Tautomers (**12** and **13**)

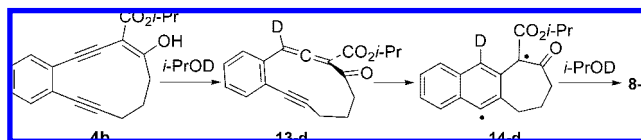
	n	ΔE (kcal/mol) ^a		d (Å) ^b	ring strain (kcal/mol) ^c
		B3LYP/6-311++G(d,p)	MP2/6-31++G(d,p)		
2a^K	1	8.0	3.9	3.38	9.9
2a^E	1	4.1	3.2	3.24	10.0
2b^K	1	6.2	1.6	3.44	7.1
2b^E	1	0.0	0.0	3.21	11.0
12	1	0.4	−0.4		7.6
4a^K	2	12.6	8.5	3.89	
4a^E	2	4.7	3.2	3.77	
4b^K	2	11.7	6.5	3.88	
4b^E	2	0.0	0.0	3.77	
13	2	4.7	3.1		

^a ZPVE-corrected energy; the electronic energies of **2b^E** and **4b^E** were used as the references for the 10- and 11-membered-ring systems, respectively. ^b Distance between acetylenic termini (see Scheme 5). ^c See the Supporting Information for details concerning the ring-strain calculations.

thermodynamic stability of tautomers **2a^E** and **2b^E** is accompanied by somewhat greater ring strain and shorter transannular distances than in corresponding keto forms. Thus, in both keto tautomers (**2a^K** and **2b^K**), d is greater than the Nicolaou “critical distance” for spontaneous cyclization of enediynes (3.31 Å),²² but it drops below that value in enol tautomers **2a^E** and **2b^E**. While cyclization of **2b** apparently proceeds via a different mechanism (see below), the enhanced reactivity of **2a** can be explained by the additional ring strain introduced by the enolic double bond. The separation between the acetylenic termini in the DFT-optimized structures of 11-membered-ring enediynes **4a^E** and **4b^E**, on the other hand, is ~ 3.77 Å. Such a distance is usually associated with a high activation barrier for Bergman cyclization.²¹ In fact, the parent cycloundeca-1,5-diyne-3-ene, for which $d = 3.661$ Å (from X-ray data²³), is stable up to 84 °C.¹⁸ The rapid cyclization of **4b**, and apparently **2b**, under ambient conditions should therefore proceed by some other (non-Bergman) mechanism. The obvious difference between the more stable (**2a**, **4a**) and reactive (**2b**, **4b**) regioisomers is the presence of a third, allenic form in the tautomeric equilibria of the latter two (**12** and **13**, respectively; see Scheme 5). The allenic tautomer **12** has virtually the same stability as the enol **2b^E** and should therefore be a prominent component of the equilibrium mixture. Allene **13** is somewhat higher in energy than the corresponding enol tautomer **4b^E** but still substantially more stable than the parent keto form **4b^K** (Table 1). The presence of **12** and **13** in the tautomeric equilibria might explain the unusually facile cyclization of enediynes **2b** and **4b**, respectively. Allene–eneynes, such as **12** or **13**, can undergo Myers–Saito cyclization, which has a substantially lower activation barrier than the Bergman reaction.^{3,24} In fact, cyclic structures containing the (Z)-1,2,4-heptatrien-6-yne fragment are unknown. In the case of **12** and **13**, the transition-state energy should be

further reduced by the delocalization of the spin of the forming π radical to the adjacent carbonyl groups. The observed formation of **8-d** in 2-propanol- d_1 (Scheme 4) agrees with isomerization/Myers–Saito cyclization pathway for the cyclization of **4b**. The tautomerization of the latter to the allenic ketone should proceed via transfer of an acidic proton from the solvent to the acetylenic carbon of **4b**. In 2-propanol- d_1 , this would result in the introduction of deuterium at the γ position with respect to the ketone moiety (**13-d** in Scheme 6). Allene–eneyne **13-d** would then undergo Myers–Saito cyclization to produce α ,3-dehydrotoluene radical **14-d**, which would proceed to abstract protium from the solvent to give the final product **8-d** (Scheme 6).

Scheme 6

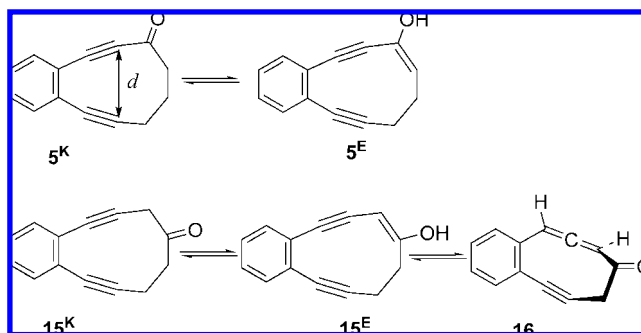


The primary kinetic isotope effect on the rate of this reaction in 2-propanol- d_1 ($k_H/k_D = 2.18$ for **4b**) indicates that rate-limiting step involves a proton transfer from the hydroxyl group of the solvent to the substrate. In other words, the overall rate of the cycloaromatization of **4b** is controlled by the tautomerization of the latter into the allenic form **13**, while the Myers–Saito step is much faster. The fact that no allenic bands are observed in FT-IR spectra of the reaction mixtures of photolyses of **7** provide additional support for this mechanistic assignment.

Several examples of enediyne cycloaromatization triggered by base-²⁵ or acid-catalyzed²⁶ acetylene–allene rearrangement have been reported. In the case of **4b**, however, such isomerization is spontaneous and does not require external reagents. We believe that the difference in the reactivities of the regioisomeric ten-membered cyclic enediynes **2a** and **2b** can be similarly explained by the fact that cyclization of **2b** proceeds via isomerization of **2b** into the allene–eneyne form **12** followed by rapid Myers–Saito cyclization, while **2a** cyclizes via a slower Bergman mechanism.

Model Studies. To explore the mechanism of enediyne cycloaromatization via β,γ -acetylenic ketone to allenic ketone tautomerization, we analyzed keto–enol equilibria of two isomeric model enediynes: 4,5-benzocyclodeca-2,6-diyne (**5**) and 5,6-benzocyclodeca-3,7-diyne (**15**) (Scheme 7). The B3LYP/6-31++G(d,p)-optimized geometries of structures **5^K**, **5^E**, **15^K**, and **15^E** as well as that of allene–eneyne **16** are provided in the Supporting Information. The relative electronic energies of tautomers and transannular distances are shown in Table 2.

Scheme 7

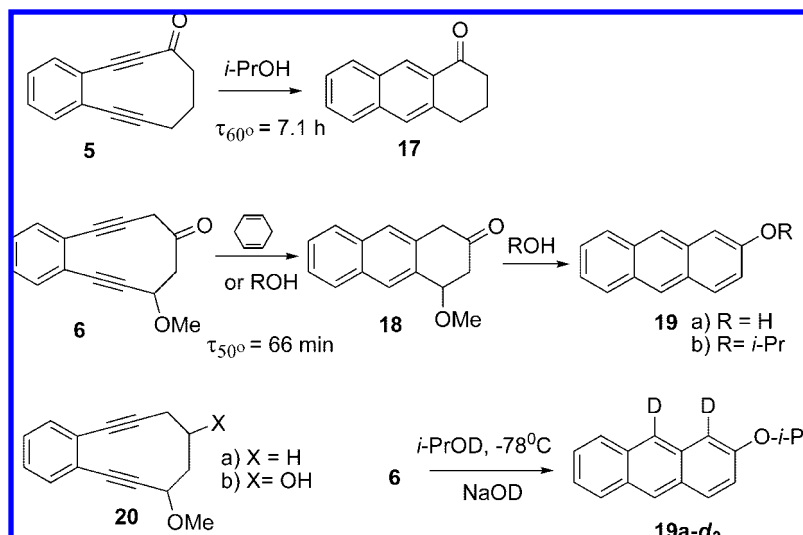


(22) Nicolaou, K. C.; Zuccarello, G.; Riemer, C.; Estevez, V. A.; Dai, W. M. *J. Am. Chem. Soc.* **1992**, *114*, 7360.

(23) Nicolaou, K. C.; Ogawa, Y.; Zuccarello, G.; Schweiger, E. J.; Kumazawa, T. *J. Am. Chem. Soc.* **1988**, *110*, 4866.

(24) (a) Schreiner, P. R.; Navarro-Vasquez, A.; Prall, M. *Acc. Chem. Res.* **2005**, *38*, 29. (b) Schmittel, M.; Steffen, J.-P.; Maywald, M.; Engels, B.; Helten, H.; Musch, P. *J. Chem. Soc., Perkin Trans. 2* **2001**, 1331. (c) Chen, W.-C.; Zou, J.-W.; Yu, C.-H. *J. Org. Chem.* **2003**, *68*, 3663.

Scheme 8



In an expected contrast to the case of the fully enolized β -ketoesters **2a**, **2b**, **4a**, and **4b**, the enol tautomers (**5^E** and **15^E**) of the two isomeric keto-enediynes **5** and **15** are predicted by DFT and MP2 methods to be higher in energy than the corresponding keto forms (**5^K** and **15^K**). Similar to the case for β -ketoesters **2** and **4**, the transannular distances are shorter in the enol forms than in the keto forms of these 10-membered-ring enediynes. The transannular distance in the DFT-optimized structure **5^K** is in good agreement with the X-ray data ($d = 3.325 \text{ \AA}$)²⁷ for this compound. The allene–eneiyne **16** is the most stable form among the three tautomers of **15** (Table 2). In an established equilibrium, **16** should be the predominant component, and the cyclization of enediyne **15** should proceed via the Myers–Saito pathway, which is not feasible for **5**.

To test these predictions experimentally, we prepared model keto-enediynes **5** and **6**.¹⁷ The methoxy substituent at the propargylic position of **6** was introduced in an attempt to offset the inductive effect of the carbonyl oxygen in the structure **5** on the rate of cycloaromatization. In good agreement with theoretical results, NMR data showed that enediynes **5** and **6** exist exclusively in their keto form. Other tautomeric forms were not detected by NMR or IR spectroscopy. When **5** and **6** are subjected to mild heating in 2-propanol, they both undergo smooth Bergman cyclization, producing 3,4-dihydro-1-(2*H*)anthracenone (**17**) and 3,4-dihydro-4-methoxy-2-(1*H*)anthracenone (**18**), respectively. The latter, however, is not very stable. When it is heated in hydroxylic solvents, on silica gel, or in the presence of trace amounts of acid or base, ketone **18** loses methanol to give 2-anthracenol derivatives **19** (Scheme 8).

While the transannular distance is expected to be somewhat longer in **6** than in **5** (compare the d values of **5^K** and **15^K** given in Table 2), it undergoes cycloaromatization much faster than **5**. The corresponding lifetimes in 2-propanol are $\tau_{50^\circ\text{C}} = 66 \text{ min}$ and $\tau_{60^\circ\text{C}} = 7.1 \text{ h}$. The reactivity of **5** is consistent with

Table 2. Relative Electronic Energies and Transannular Distances for Keto and Enol Forms of 10-Membered-Ring Keto-Enediynes (**5** and **15**) and for the Corresponding Enyne–Allene Tautomer (**16**)

	ΔE (kcal/mol) ^a		d (\AA) ^b
	B3LYP/6-311++G(d,p)	MP2/6-31++G(d,p)	
5^K	8.1	4.8	3.37
5^E	19.2	17.0	3.23
15^K	5.2	1.4	3.42
15^E	13.7	11.9	3.20
16	0.0	0.0	

^a ZPVE-corrected energy; the energy of allene–eneiyne **16** was used as the reference. ^b Distance between acetylenic termini (see Scheme 7).

that reported previously ($\tau_{40^\circ\text{C}} = 82 \text{ h}$ in $\text{C}_6\text{D}_6/1,4\text{-cyclohexadiene}$).²⁸ Cycloaromatization of enediyne **6** is also substantially faster than that of the parent compound **20a** ($\tau_{60^\circ\text{C}} = 36.5 \text{ h}$ in 1,4-cyclohexadiene)²⁹ or the alcohol precursor **20b** ($\tau_{50^\circ\text{C}} = 22 \text{ h}$ in 2-propanol) (Scheme 8).¹⁷ The observed high reactivity of **6** agrees well with the proposed tautomerization to **16**/Myers–Saito cyclization pathway, which is not available to **5**. Results of isotope-labeling experiments support this mechanism. Treatment of a 2-propanol- d_1 solution of **6** with catalytic amounts of NaOD at -78°C produces 2-anthracenol with 75% deuteration at the 9 position (**19a-d₂**, Scheme 8). Since abstraction of deuterium from the solvent by a 1,4-naphthyl diradical (similar to **11** in Scheme 4) is highly unlikely (see above), isotopic substitution at the 9 position apparently occurs during ketonization of **15^E** to **16**. The second deuterium at the 1 position is apparently incorporated via base-catalyzed proton exchange α to the carbonyl group of **18**.

Acid–base catalysis of the cycloaromatization reaction of enediyne **6** was studied in wholly aqueous solutions. Preparative experiments using 5% 2-propanol as the cosolvent allowed us to isolate 2-anthracenol (**19a**) in 75–80% yield under both acidic and basic conditions. The formation of **18** and subsequent conversion to **19a** was followed spectroscopically using the characteristic absorbance of **18** at 228 nm (Figure 2). Measurements were made at $40 \pm 0.1^\circ\text{C}$ with either a Cary 300 UV spectrometer or, for the faster reactions in basic solutions, a

(25) (a) Grissom, J. W.; Klingberg, D. *Tetrahedron Lett.* **1995**, *36*, 6607. (b) Baba, G.; Tea, C. G.; Toure, S. A.; Lesvier, M.; Denis, J. M. *J. Organomet. Chem.* **2002**, *643*, 342.

(26) (a) Naoe, Y.; Kikuchi, J.; Ishigaki, K.; Iitsuka, H.; Nemoto, H.; Shibuya, M. *Tetrahedron Lett.* **1995**, *36*, 9165. (b) Suzuki, I.; Wakayama, M.; Shigenaga, A.; Nemoto, H.; Shibuya, M. *Tetrahedron Lett.* **2000**, *41*, 10019. (c) Suzuki, I.; Shigenaga, A.; Nemoto, H.; Shibuya, M. *Heterocycles* **2001**, *54*, 571.

(27) Cousson, A.; Dancy, I.; Beau, J.-M. *Acta Crystallogr.* **1995**, *C51*, 718.

(28) Semmelhack, M. F.; Neu, T.; Foubelo, F. *J. Org. Chem.* **1994**, *59*, 5038.

(29) Boger, D. L.; Zhou, J. *J. Org. Chem.* **1993**, *58*, 3018.

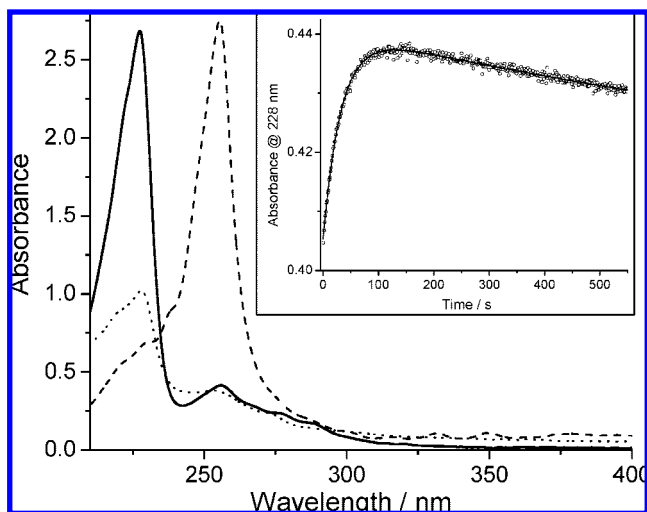


Figure 2. UV spectra of $\sim 4 \times 10^{-5}$ M 2-propanol solutions of (dotted line) **6**, (solid line) **18**, and (dashed line) **19a**. The inset shows part of the kinetic curve at 228 nm in biposphate buffer (BR = 0.74). The line was drawn using parameters obtained by least-squares fitting of a double-exponential equation.

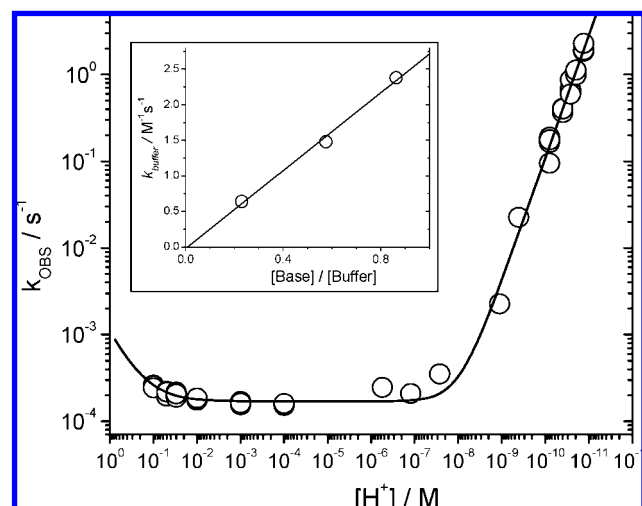
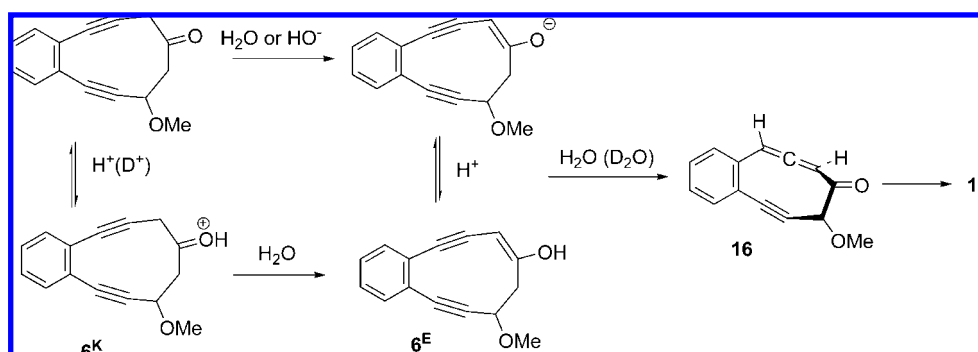


Figure 3. Rate profile for the cycloaromatization of enediyne **6** in aqueous solution at 40 °C. The inset shows the dependence of the buffer catalysis on the fraction of basic component of the buffer.

Cary 50 spectrometer equipped with a stopped-flow attachment. A portion of a typical kinetic curve is shown in Figure 2.

Rates of cyclization of **6** were determined in dilute aqueous solutions of perchloric acid and sodium hydroxide as well as

Scheme 9



in biphosphate ion, bicarbonate ion, and TRIS buffers. The kinetic data obeyed the first-order rate law well, and the observed pseudo-first-order rate constants were determined by least-squares fitting to a double-exponential function.

The isomerization reaction proved to be strongly catalyzed by all of the buffers examined. Therefore, measurements were consequently performed in series of solutions with constant buffer ratio (BR = [acid]/[base]) but varying buffer concentration. The observed rates were extrapolated to zero buffer concentration.¹⁷ These buffer-independent rate constants, together with observed rate constants determined in perchloric acid and sodium hydroxide solutions, are shown as the rate profile in Figure 3.

This rate profile shows a horizontal region between pH 2 and pH 7, in which the rate constant $k_{\text{H}_2\text{O}}$ has the value $(1.7 \pm 0.5) \times 10^{-4} \text{ s}^{-1}$ and is independent of the acidity of the medium. The reaction is strongly catalyzed by base, as illustrated by the upward slope of the rate profile above pH 8. The hydroxide ion catalysis measured in NaOH solutions is characterized by the second-order rate constant $k_{\text{OH}^-} = 1509 \pm 88 \text{ M}^{-1} \text{ s}^{-1}$. There is also a region of weak acid catalysis below pH 3, with rate constant $k_{\text{H}^+} = (9.3 \pm 0.7) \times 10^{-4} \text{ M}^{-1} \text{ s}^{-1}$. It is important to note that the rate of conventional Bergman cyclization is independent of the acid concentration.³⁰ The slopes of biphosphate buffer-dilution plots ($k_{\text{cat}} = 2.38 \pm 0.06$, 1.48 ± 0.04 , and $0.64 \pm 0.03 \text{ M}^{-1} \text{ s}^{-1}$ for BR = 1/6, 5/7, and 10/3, respectively) represent pH-independent catalysis by the buffer components. These can be partitioned into contributions from the acidic and basic components of the buffer by plotting k_{cat} against the fraction of base component in the buffer ($f_{\text{B}} = [\text{base}]/[\text{buffer}]$), as illustrated in the inset in Figure 3. As k_{cat} extrapolates to zero at $f_{\text{B}} = 0$ and has a value of $2.72 \pm 0.10 \text{ M}^{-1} \text{ s}^{-1}$ at $f_{\text{B}} = 1$, we can conclude that cycloaromatization of **6** is strongly catalyzed by general base but shows no general acid catalysis. These features can be accommodated by the reaction mechanism shown in Scheme 9, in which cycloaromatization occurs through the rate-limiting enolization of ketone **6^K** (or its protonated form at low pH). Below pH 8, water serves as the base, removing a proton from the α position with respect to the carbonyl group of the substrate, while at higher pH, hydroxide ion takes over as the deprotonating agent. Strong general base catalysis is characteristic for reactions proceeding via the rate-limiting C–H deprotonation step. Specific acid catalysis is another common feature of enolization reactions, because O-protonation of ketones increases their C–H acidity and the rate of tautomerization. The enol or enolate form of **6** is reprotonated in the γ position to produce allene **16**. The latter then undergoes facile Myers–Saito cyclization to afford ketone **18**.

Rates of the cycloaromatization of **6** were also measured in dilute DCl solutions in D₂O. The observed solvent isotope effect agrees well with the rate-limiting enolization. At very low DCl concentrations, the reaction was slower in D₂O, producing a secondary isotope effect $k_{\text{H}_2\text{O}}/k_{\text{D}_2\text{O}} \approx 1.4$ in the normal direction. At this pH, water acts as a base, accepting proton from **6^K** (Scheme 9) to become a hydronium ion. This is a bond-loosening process that gives a secondary isotope effect in the normal direction ($k_{\text{H}}/k_{\text{D}} > 1$).³¹ On the other hand, the slope of DCl catalysis is almost twice as steep as that of HClO₄ ($k_{\text{H}^+}/k_{\text{D}^+} \approx 0.6$). This inverse isotope effect is due to the fact that acids are weaker in D₂O, so the fraction of the more reactive protonated species **6^K** grows faster with D⁺ concentration than with H⁺ concentration.³¹ The absence of a primary kinetic isotope effect on the cyclization of **6** in D₂O shows that reprotonation in the γ position (i.e., ketonization to allene **16**) of **6^E** is much faster than enolization. Clean exponential growth of the absorbance at 228 nm indicates that conversion of **6** to **18** proceeds without significant accumulation of intermediates (e.g., **15^E** or **16**). This observation allows us to conclude that cyclization of allene–ene-yne **16** is much faster than the tautomerization step. Since the rate constant of the overall process in basic solutions approaches 10 s⁻¹, we can estimate the upper limit for the lifetime of **16** at 40 °C as ~ 100 ms.

Conclusions

The rates of cycloaromatization of cyclic 10- and 11-membered-ring enediynes can be substantially enhanced by introducing a carbonyl group in the β position with respect to the acetylenic terminus. Cyclization of such β -keto enediynes

proceeds via tautomerization into the more reactive allene–ene-yne, which then undergoes facile Myers–Saito cyclization. Cycloaromatization of 8-methoxy-5,6-benzocyclodeca-3,7-diyne (**6**) is weakly catalyzed by hydronium ion and shows strong general base catalysis. These observations, along with the values of the solvent isotope effect, indicate that enolization to **6^E** is the rate-limiting step in the cyclization of **6**. Unstable α -carbalkoxy- β -keto enediynes **2a** and **4a** apparently already exist in enol form. The rates of their cycloaromatization show significant primary isotope effects, suggesting that enol–keto–allene tautomerization controls the overall rate of the reaction, while Myers–Saito cyclization of the allene is much faster. The lifetime of 10-membered-ring allene–ene-yne **16** at 40 °C is less than 100 ms. Since the rate of enolization and the position of the keto–enol equilibrium depends on the pH of the solution, the presence of various cations, and other factors, this design opens a new approach for controlling enediyne reactivity.

Acknowledgment. The authors thank the National Science Foundation (CHE-0449478), Georgia Cancer Coalition, and donors of the ACS Petroleum Research Fund (434444-AC4) for support of this project.

Supporting Information Available: Experimental details; synthetic procedures for the preparation of compounds **5**, **6**, and **7**; isolation and characterization of reaction products; and Cartesian coordinates of DFT-optimized structures. This material is available free of charge via the Internet at <http://pubs.acs.org>.

JA802688C

(30) Perrin, C. L.; Rodgers, B. L.; O'Connor, J. M. *J. Am. Chem. Soc.* **2007**, *129*, 4795.

(31) Kresge, A. J.; More O'Ferrall, R. A.; Powell, M. F. In *Isotopes in Organic Chemistry*; Buncl, E., Lee, C. C., Eds.; Elsevier: New York, 1987; Vol. 7, Chapter 4.